Life Sciences 237 (2019) 116944

Contents lists available at ScienceDirect

Life Sciences

journal homepage: www.elsevier.com/locate/lifescie

The PERK/Nrf2 pathway mediates endoplasmic reticulum stress-induced injury by upregulating endoplasmic reticulophagy in H9c2 cardiomyoblasts

Tianqi Tao, Jianli Wang, Xiaoreng Wang, You Wang, Huimin Mao, Xiuhua Liu*

Department of Pathophysiology, Chinese PLA General Hospital, Beijing, China

ARTICLE INFO

Keywords:
H9c2 cell
Endoplasmic reticulophagy
Endoplasmic reticulum stress
Protein kinase R-like ER kinase
Nuclear factor erythroid 2-related factor 2

ABSTRACT

Aims: Endoplasmic reticulum stress (ERS) is an evolutionarily conserved cell stress response. Recently, it was found that ERS induces not only apoptosis but also endoplasmic reticulophagy (ER-phagy). A previous study demonstrated that inhibition of ER-phagy alleviates cell injury. The purpose of this study was to investigate the involvement of the protein kinase R-like ER kinase (PERK)/nuclear factor erythroid 2-related factor 2 (Nrf2) pathway in ERS-induced ER-phagy in H9c2 cardiomyoblasts. To address this aim, cells were treated with ERS inhibitors and a Nrf2 inhibitor before establishment of thapsigargin (TG)- or tunicamycin (TM)-induced ERS models in H9c2 cardiomyoblasts.

Main methods: Transmission electron microscopy and immunofluorescence staining were used to detect ER-phagy. Western blotting was employed to detect the levels of calreticulin (CRT), total and phosphorylated PERK, nuclear Nrf2, activated transcription factor 4 (ATF4), light chain 3B (LC3B)-II and Beclin 1. Immunofluorescence staining was used to assess subcellular location of Nrf2.

Key finding: TG or TM induced H9c2 cell injury and ER-phagy and upregulated CRT expression, PERK phosphorylation, Nrf2 nuclear translocation, and expression of ATF4, Beclin 1, and LC3B-II compared with control cells. Treatment with ERS inhibitors decreased TG- or TM-induced ER-phagy, downregulated CRT expression, PERK phosphorylation, Nrf2 nuclear translocation and the expression of ATF4, Beclin 1 and LC3B-II. Moreover, a Nrf2 inhibitor downregulated the expression of ATF4, Beclin 1 and LC3B-II and alleviated TG- or TM-induced ER-phagy and H9c2 cell injury.

Significance: These findings suggest that the PERK/Nrf2 pathway mediates upregulation of ER-phagy, thereby inducing cell injury in H9c2 cardiomyoblasts.

1. Introduction

Cardiovascular disease (CVD) remains the leading cause of morbidity and mortality worldwide and is responsible for a huge societal burden and cost. Many conditions, such as myocardial ischemia/reperfusion injury, can lead to an increase in cardiomyocyte autophagy [1]. Moderate autophagy promotes cardiomyocyte survival in the injured myocardium by eliminating damaged organelles; however, excessive autophagic activation seems to trigger cell death, which contributes to major cardiovascular disorders [2]. Recently, it has been found that autophagy also appears to operate in an organelle-selective manner, such as endoplasmic reticulophagy (ER-phagy) [3], mitophagy [4] and lipophagy [5]. ER-phagy is a phenomenon of selective autophagy of endoplasmic reticulum (ER) involving the formation of ER-containing autophagosomes (ERAs) and was discovered by Bernales in 2007 [3]. ER-phagy degrades the redundant ER membranes and maintains cell homeostasis [6,7]. It has been reported that excessive ER-phagy caused cell injury in HeLa cells and human embryonic kidney cells [8,9], suggesting that downregulating ER-phagy might have a protective role in cells. Further studies have confirmed that endoplasmic reticulum stress (ERS) can directly induce ER-phagy, but the mechanism by which ERS causes ER-phagy in cardiomyocytes has not been investigated.

ERS is mediated by the activation of three major stress sensors: protein kinase RNA-like ER kinase (PERK), inositol-requiring protein 1 (IRE1) and activating transcription factor 6 (ATF6). The PERK pathway is the immediate early-response pathway among the three ERS pathways [10]. During activation, PERK phosphorylates eukaryotic initiator factor 2α (eIF2α) to promote activating transcription factor 4 (ATF4) translation and then upregulates light chain 3 (LC3), which participates in elongation and maturation of autophagosomes. Moreover, LC3B interacts with ER-resident receptors [11] and specifically recognizes and

* Corresponding author. Department of Pathophysiology, Chinese PLA General Hospital, 28 Fuxing Road, Beijing, 100853, China.
E-mail address: xiuhualiu98@163.com (X. Liu).

https://doi.org/10.1016/j.lfs.2019.116944
Received 5 August 2019; Received in revised form 30 September 2019; Accepted 7 October 2019
Available online 08 October 2019
0024-3205/

recruits the ER into the autophagosome, which results in ER-phagy [12]. It has been suggested that the PERK pathway might contribute to ER-phagy. In addition, the PERK pathway regulates induction and nucleation of the phagophore by activating Beclin 1 [13].

A recent study demonstrated that IRE1α deficiency activated PERK-dependent autophagy and cell injury, while the expression of eIF2α, a classic downstream molecule of PERK, was downregulated [14], suggesting that another molecule mediates ER-phagy with the activation of PERK. Nuclear factor E2-related factor 2 (Nrf2), a basic leucine zipper (bZIP) protein, was previously thought to protect against oxidative stress [15]. However, recently, it has been found that Nrf2 is also an important downstream factor of PERK. PERK activates Nrf2, which then translocates into the nucleus [10]. Other studies have indicated that Nrf2 regulates ATF4 expression [16,17], suggesting that the PERK/Nrf2/ATF4 pathway might be involved in ER-phagy. Therefore, we hypothesized that the PERK/Nrf2/ATF4 pathway might mediate ERS-induced injury by upregulating ER-phagy. Our study found that the PERK/Nrf2 pathway mediates ER-phagy-induced injury by upregulating LC3B and Beclin 1 in H9c2 cardiomyoblasts.

2. Materials and methods

2.1. Antibodies and reagents

The embryonic rat cardiomyocyte-derived cell line H9c2 was purchased from American Type Culture Collection (ATCC, Manassas, VA, USA, CRL-1446). Dulbecco's modified Eagle's medium (DMEM) was purchased from Gibco (Grand Island, NY, USA), and newborn calf serum (NCS) was obtained from PAA (Pasching, Austria). Trypsin was purchased from Amresco (Solon, OH, USA). Taurine, ATRA, protease inhibitor, penicillin/streptomycin and Triton X-100 were obtained from Sigma (St Louis, MO, USA). Thapsigargin (TG), tauroursodeoxycholic acid (TUDCA), phosphatase inhibitor and bovine serum albumin (BSA) were obtained from Merck (Rahway, NJ, USA). Tunicamycin (TM); rabbit polyclonal antibodies against CRT, PERK, LC3B and Beclin 1; and rabbit monoclonal antibody against histone H3 and glyceraldehyde-3-phosphate dehydrogenase (GAPDH) were purchased from Cell Signaling Technology (Danvers, MA, USA). Rabbit polyclonal antibodies against phosphorylated PERK (p-PERK), Nrf2, and ATF4; goat monoclonal antibody against CRT; Texas red-conjugated donkey anti-rabbit secondary antibody; FITC-conjugated donkey anti-goat secondary antibody; and enhanced chemiluminescence (ECL) reagents were from Santa Cruz Biotechnology (Santa Cruz, CA, USA). Horseradish peroxidase (HRP)-conjugated goat anti-rabbit immunoglobulin G (IgG) was from Epitomics (Burlingame, CA, USA). The CCK-8 detection kit was from Dojindo Molecular Technologies, Inc. (Kumamoto-ken, Kyushu, Japan). The LIVE/DEAD® Viability/Cytotoxicity Kit and NE-PER Nuclear and Cytoplasmic Extraction Kit were from Thermo Fisher Scientific (Waltham, MA, USA). The mounting medium with DAPI was from Vector Laboratories (Burlingame, CA, USA).

2.2. Cell culture and experiment protocol

H9c2 cardiomyoblasts were used as a model because they mimic the hypertrophic responses of primary rat neonatal cardiomyocytes in vitro [18]. H9c2 cardiomyoblasts were cultured in high-glucose DMEM supplemented with 10% fetal bovine serum (FBS) and an antibiotic-antimycotic solution, placed into T-25 flasks with the same medium, and incubated at 37 °C with 5% CO_2. Following 24 h, the cells were transferred to serum-free maintenance medium (DMEM containing 1% penicillin/streptomycin) for 12 h before experimentation. To evaluate the protective effects of ERS inhibitors (taurine and tauroursodeoxycholic acid) against ERS-induced (by TG or TM) ER-phagy, H9c2 cardiomyoblasts were divided into 9 groups: (1) control group, H9c2 cardiomyoblasts were cultured in a 5% CO_2 incubator at 37 °C for 48 h; (2) Tau group, incubation with 40 mmol/L taurine for 48 h; (3) TUDCA group, incubation with 500 μmol/L tauroursodeoxycholic acid for 48 h; (4) TG group, incubation with 20 nmol/L thapsigargin for 48 h [19]; (5) Tau + TG group, incubation with 40 mmol/L taurine [20] and 20 nmol/L thapsigargin for 48 h; (6) TUDCA + TG group, pretreatment with 500 μmol/L TUDCA for 1 h [21,22] followed by incubation with 20 nmol/L thapsigargin for 48 h; (7) TM group, incubation with 160 ng/mL tunicamycin for 48 h [19]; (8) Tau + TM group, incubation with 40 mmol/L taurine [20] and 160 ng/mL tunicamycin for 48 h; (9) TUDCA + TM group, pretreatment with 500 μmol/L TUDCA for 1 h [21,22] followed by incubation with 160 ng/mL tunicamycin for 48 h.

To further evaluate the role of the PERK/Nrf2 pathway in regulating ER-phagy, we treated H9c2 cardiomyoblasts with ATRA, a Nrf2 nuclear translocation inhibitor [23,24]. The experimental groups were as follows: (1) control group, H9c2 cardiomyoblasts remained in a 5% CO_2 incubator at 37 °C as before; (2) ATRA group, incubation with 20 nmol/L ATRA for 48 h; (3) TG group, incubation with 20 nmol/L thapsigargin for 48 h; (4) ATRA + TG group, pretreatment with 20 nmol/L ATRA for 24 h followed by incubation with 20 nmol/L TG for 48 h; (5) TM group, incubation with 160 ng/mL TM for 48 h; (6) ATRA + TM group, pretreatment with 20 nmol/L ATRA for 24 h followed by incubation with 160 ng/mL TM for 48 h.

2.3. Preparation of whole and nuclear proteins and Western blot analysis

H9c2 cardiomyoblasts were plated in T-25 flasks at 5×10^5 cells per flask. H9c2 cardiomyoblasts were collected with 0.25% trypsin containing EDTA. Proteins were extracted from H9c2 cardiomyoblasts with lysis buffer containing a protease inhibitor and phosphatase inhibitor. The entire process was performed on ice. Equal amounts of protein (80 μg/lane as determined by Bradford analysis) were resolved on 10% sodium dodecyl sulfate-polyacrylamide gels. After electrophoresis, proteins were electrophoretically transferred to nitrocellulose membranes. The membranes were blocked with 5% BSA in Tris-buffered saline containing 0.1% Tween 20 (TBS-T) at 4 °C for 4 h. Then, the membranes were probed with primary antibodies against PERK, GAPDH, histone H3 (all 1:1000 diluted), Nrf2 (1:100 diluted), CRT, ATF4, p-PERK, LC3B and Beclin 1 (all 1:500 diluted) at 4 °C overnight. The antibody-tagged membrane was incubated with a secondary antibody solution consisting of a 1:1000 dilution of HRP-conjugated goat anti-rabbit IgG (for CRT, PERK, p-PERK, Nrf2, ATF4, LC3B, Beclin 1, GAPDH, and histone H3). An enhanced chemiluminescence detection system was used for immunoblot protein detection. The optical density of the bands (as measured in arbitrary densitometry units) was determined using Image-Pro Plus (Roper Industries, New York, NY, USA), and the densitometry of the immunoblots was normalized against GAPDH. In addition, the nuclear Nrf2 protein level was obtained using NE-PER Nuclear and Cytoplasmic Extraction Reagents, and the nuclear protein densitometry was normalized against histone H3.

2.4. Assessment of cell viability

CCK-8 detection is a method for estimating cell viability. Cells were plated in 96-well plates at 5×10^3 cells per well. We added 10 μl CCK-8 into 90 μl DMEM in each well, with 8 compound wells in each group (n = 3), and then incubated the cells at 37 °C for 2 h. Samples were measured using a microplate reader at a wavelength of 450 nm (Tecan Infinite f200 Pro; Tecan Group Ltd., Männedorf, Switzerland).

2.5. Assessment of cell death

The LIVE/DEAD® Viability/Cytotoxicity Assay Kit provides a two-color fluorescence assay that is based on simultaneous determination of live and dead cells with two probes. Live cells are distinguished by the nonfluorescent cell-permeant dye calcein AM, which produces a green fluorescence in live cells. Ethidium homodimer-1 (EthD-1) enters

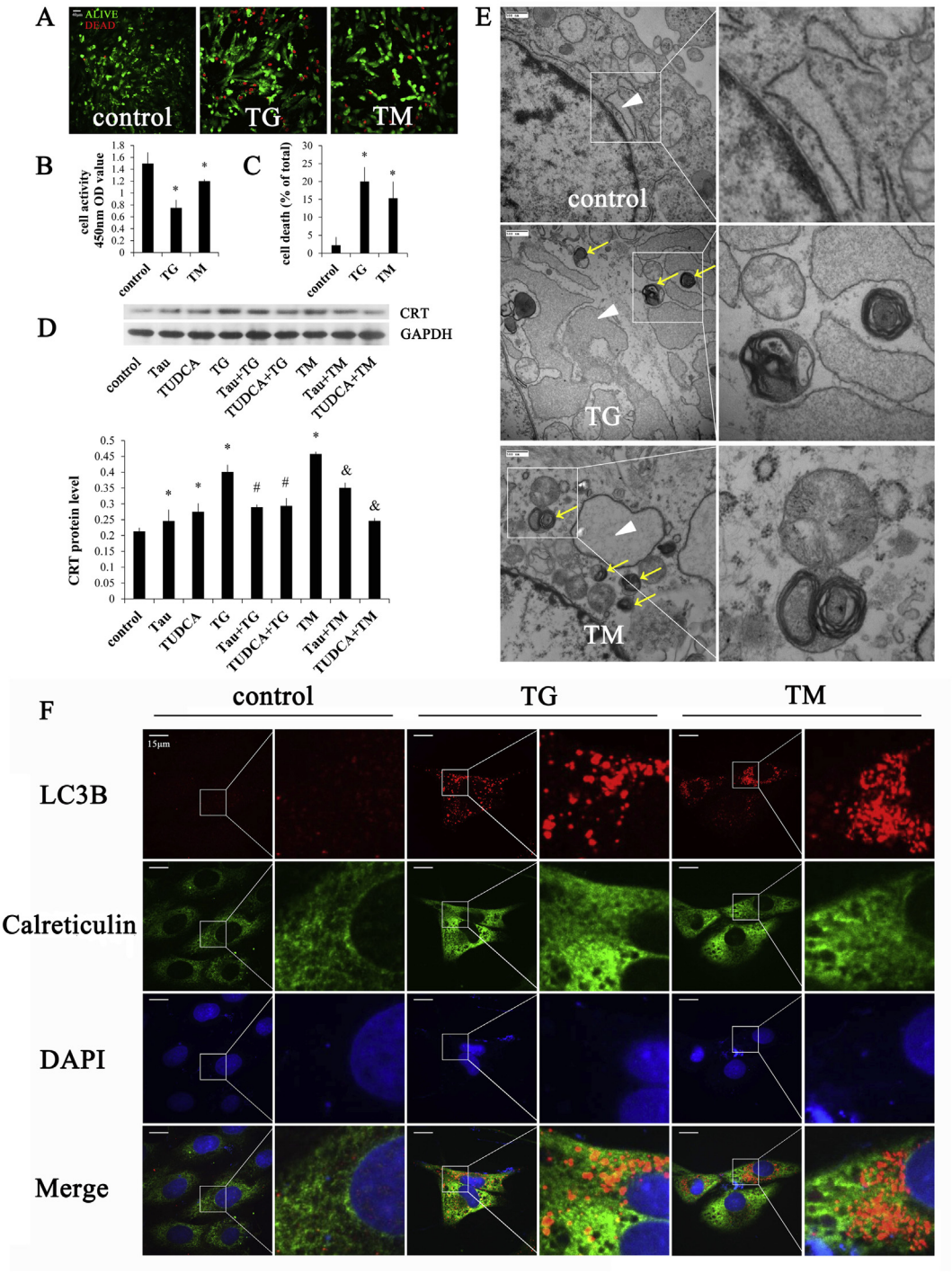

Fig. 1. ERS caused ER-phagy with a decrease in cell viability and an increase in cell death in H9c2 cardiomyoblasts. (A) Live/Dead staining of H9c2 cardiomyoblasts was performed using a LIVE/DEAD® Viability/Cytotoxicity Kit (bar = 40 μm). TG- or TM-treated H9c2 cardiomyoblasts were incubated with calcein-AM (green) and EthD-1 (red) for 10 min, and the fluorescence was visualized using a confocal microscope. Green fluorescence indicates live cells, while red fluorescence indicates dead cells. (B) The viability of TG- or TM-treated H9c2 cardiomyoblasts was detected with a CCK-8 assay. (C) Quantitative analysis of live (green) and dead (red) H9c2 cardiomyoblasts treated with TG or TM as shown in (A). (D) Western blotting was used to detect the effects of Tau and TUDCA on expression of the ERS-related molecule CRT after TG or TM treatment. (E) Ultrastructural lesions in the ER caused by TG or TM and the occurrence of ER-phagy were observed via transmission electron microscopy (bar = 500 nm). White arrows indicate the ER, and yellow arrows indicate ERAs (with ER whorls). The pictures on the right show amplified regions of the panels containing ERAs, control to TM. (F) Representative confocal microscopy images corresponding to analysis of ER-phagy for TG- or TM-treated H9c2 cardiomyoblasts and showing colocalization of autophagosomes with ER-fragments (bar = 15 μm). LC3B was labeled with Texas Red, while calreticulin was labeled with Alexa Fluor 488. Our experiments were done in triplicate. The data were analyzed via one-way analysis of variance and are shown as the mean ± standard deviation (SD) of three independent biological replicates in (B), (C) and (D). $^{*}P < 0.05$ versus control, $^{\#}P < 0.05$ versus TG, $^{\&}P < 0.05$ versus TM. (For interpretation of the references to color in this figure legend, the reader is referred to the Web version of this article.)

through damaged membranes and binds to nucleic acids, producing a red fluorescence in dead cells. The detection methods were as follows: the cells were cultured on coverslips at a density of $2 \times 10^4/cm^2$. Cells were washed twice gently with 0.1 mol/L PBS and a mixture of 4 μmol/L EthD-1 and 2 μmol/L calcein AM was added into each sample, which was then incubated at room temperature for 10 min. Cell death was measured by counting the number of dead and total cells in 3 or 5 visual fields (approximately 100–200 cells per visual field) via laser scanning confocal microscopy (UltraVIEW VoX, PerkinElmer, US). A 10 × objective with a numerical aperture of 0.3 was used.

2.6. Transmission electron microscopy

H9c2 cardiomyoblasts were plated in T-75 flasks at 1.5×10^6 cells per flask. Cells were washed with 0.1 mol/L PBS, harvested with a cell scraper, and then centrifuged at 3000 rpm for 30 s. Cells were fixed with 2.5% glutaraldehyde at 4 °C for 2 h, and then, the samples were subjected to acetone gradient dehydration, Epon812 embedding, semithin section optical positioning, and ultrathin sectioning. The sections were double-stained with uranyl acetate and lead citrate. Ultrastructure was examined using an H-7650 transmission electron microscope (10000 × ; Hitachi7650 TEM, Tokyo, Japan). More than eight images per group were obtained randomly with the transmission electron microscope.

2.7. Immunofluorescence staining

H9c2 cardiomyoblasts were grown on coverslips coated with NCS at a density of 2×10^4 cells/cm^2. After treatment, H9c2 cardiomyoblasts were fixed in 4% paraformaldehyde at room temperature for 25 min and then blocked in 10% donkey serum in phosphate-buffered saline containing 1% BSA and 0.2% Triton X-100 for 50 min. We identified cells via indirect immunofluorescence staining with *anti*-Nrf2 rabbit polyclonal antibody (1:50), *anti*-CRT goat polyclonal antibody (1:100) and *anti*-LC3B rabbit polyclonal antibody (1:100) overnight at 4 °C followed by incubation with Texas red-conjugated donkey anti-rabbit and FITC-conjugated donkey anti-goat secondary antibodies (1:100) for 1 h at room temperature in the dark. The coverslips were mounted on glass slides with mounting medium. Images were acquired using a confocal scanning microscope (UltraVIEW VoX, PerkinElmer, US). The fluorescence intensity in images were analyzed using Volocity software. More than eight images per group were randomly acquired via immunofluorescence microscopy, and more than 65% of the investigated cells were found to exhibit a change in subcellular distribution of the detected molecules, as shown in figures. A 63 × oil immersion objective with a numerical aperture of 1.4 was used.

2.8. Statistical analysis

SPSS v13.0 software (Chicago, IL, USA) was used for statistical analysis. For multiple-group comparisons, one-way analysis of variance (ANOVA) followed by a Newman-Keuls post hoc analysis was performed. Values are presented as the mean ± SD. $P < 0.05$ was considered statistically significant.

3. Results

3.1. ERS inducers caused ERS-related ER-phagy

Cell injury in TG- or TM-treated H9c2 cardiomyoblasts—ERS was induced by thapsigargin (TG), which depletes Ca^{2+} from the ER, and tunicamycin (TM), which inhibits protein N-linked glycosylation [19,25]. TG or TM induced ERS-related cardiomyocyte death, which is closely related to cardiomyocyte death in cardiac diseases such as myocardial ischemia/reperfusion injury [26,27]. According to our preliminary experiment, cell injury was induced in H9c2 cardiomyoblasts by treatment with 20 nmol/L TG or 160 ng/mL TM for 48 h. Cell viability was detected with a Cell Counting Kit-8 (CCK-8) assay, and cell death was detected with a LIVE/DEAD® Viability/Cytotoxicity Kit (Fig. 1A–C). Compared with controls, TG or TM treatment decreased cell activity by 49.8% or 19.9% and increased cell death by 8.0- or 5.9-fold, respectively ($P < 0.01$). These results indicate that both TG and TM can induce a decrease in cell viability and an increase in cell death.

TG or TM induced ERS in H9c2 cardiomyoblasts—Calreticulin (CRT) is a Ca^{2+}-binding protein and a molecular chaperone in the ER lumen and regulates ER homeostasis [28]. ERS was induced by 20 nmol/L TG or 160 ng/mL TM for 48 h. Using immunoblot analysis, alterations in CRT expression were detected (Fig. 1D). It was found that TG or TM treatment increased CRT expression by 88.4% or 115% compared with controls, respectively ($P < 0.01$). These results suggest that both TG and TM can induce ERS.

TG or TM induced ER-phagy in H9c2 cardiomyoblasts—We sought to investigate the effects of ERS on ER-phagy. We examined the ultrastructure of H9c2 cardiomyoblasts treated with TG or TM via transmission electron microscopy (Fig. 1E). H9c2 cardiomyoblasts in the control group displayed normal cellular features with a normal ultrastructure of the ER. After TG or TM treatment, H9c2 cardiomyoblasts showed obvious ultrastructural lesions, including ER dilation and expansion (shown by the white triangle) and several autophagosomes (shown by the yellow arrow) compared with controls. Autophagosomes next to the ER region, which contain ER membrane twisting as whorls (ER whorls), showed nearly no cytoplasm between ER whorls and the enveloping vacuolar membrane, suggesting that the engulfment was highly selective. The diameter of the ER whorl was approximately 200–400 nm, which was consistent with previous studies [6,29].

In addition, according to a method reported previously [30], we also studied ER-phagy by observing the subcellular distribution of the autophagy marker LC3B and the ER marker calreticulin. An immunofluorescence assay was used to detect the localization of LC3B in the ER to study ER-phagy induced by TG or TM (Fig. 1F). Under TG or TM treatment, LC3B accumulated and co-localized in the ER, with the formation of clusters with high fluorescence, compared with the control group. These results suggest that ERS inducers can significantly induce ER-phagy.

3.2. ERS inhibitors alleviated ERS-induced ER-phagy

ERS inhibitors alleviated TG- or TM-induced ERS—Taurine (Tau) and tauroursodeoxycholic acid (TUDCA) are classic inhibitors of ERS [20–22]. The effect of Tau or TUDCA on expression of the ERS-related molecule CRT was detected with western blotting (Fig. 1D). Compared with controls, TG or TM induced ERS with an increase in CRT expression. Tau or TUDCA alone increased CRT expression by 15.4% and 29.2%, respectively ($P < 0.01$ vs. control), but Tau or TUDCA attenuated TG- or TM-induced ERS. Tau or TUDCA decreased TG-treated CRT expression by 27.9% and 26.8% ($P < 0.01$) and downregulated TM-treated CRT expression by 23.4% and 46.2% ($P < 0.01$), respectively. These data indicate that ERS inhibitors attenuate TG- or TM-induced ERS.

ERS inhibitors attenuated TG- or TM-induced H9c2 cell injury—The effect of Tau or TUDCA on cell viability and cell death induced by TG or TM was detected with a CCK-8 assay and a LIVE/DEAD® Viability/Cytotoxicity Kit (Fig. 2A–C). Compared with controls, TG or TM treatment decreased cell activity by 53.2% and 28.9% and increased cell death by 10.5- or 6.8-fold, respectively ($P < 0.01$). Tau or TUDCA treatment alone had no significant effect on cell viability and cell death ($P > 0.05$). However, Tau or TUDCA prior to TG or TM treatment attenuated the TG- or TM-induced cell viability decrease, exhibiting a 48.3% or 35.1% increase compared with the TG group alone and a 23.6% or 33.5% increase compared with the TM group alone, respectively ($P < 0.01$). Moreover, Tau or TUDCA followed by TG or TM

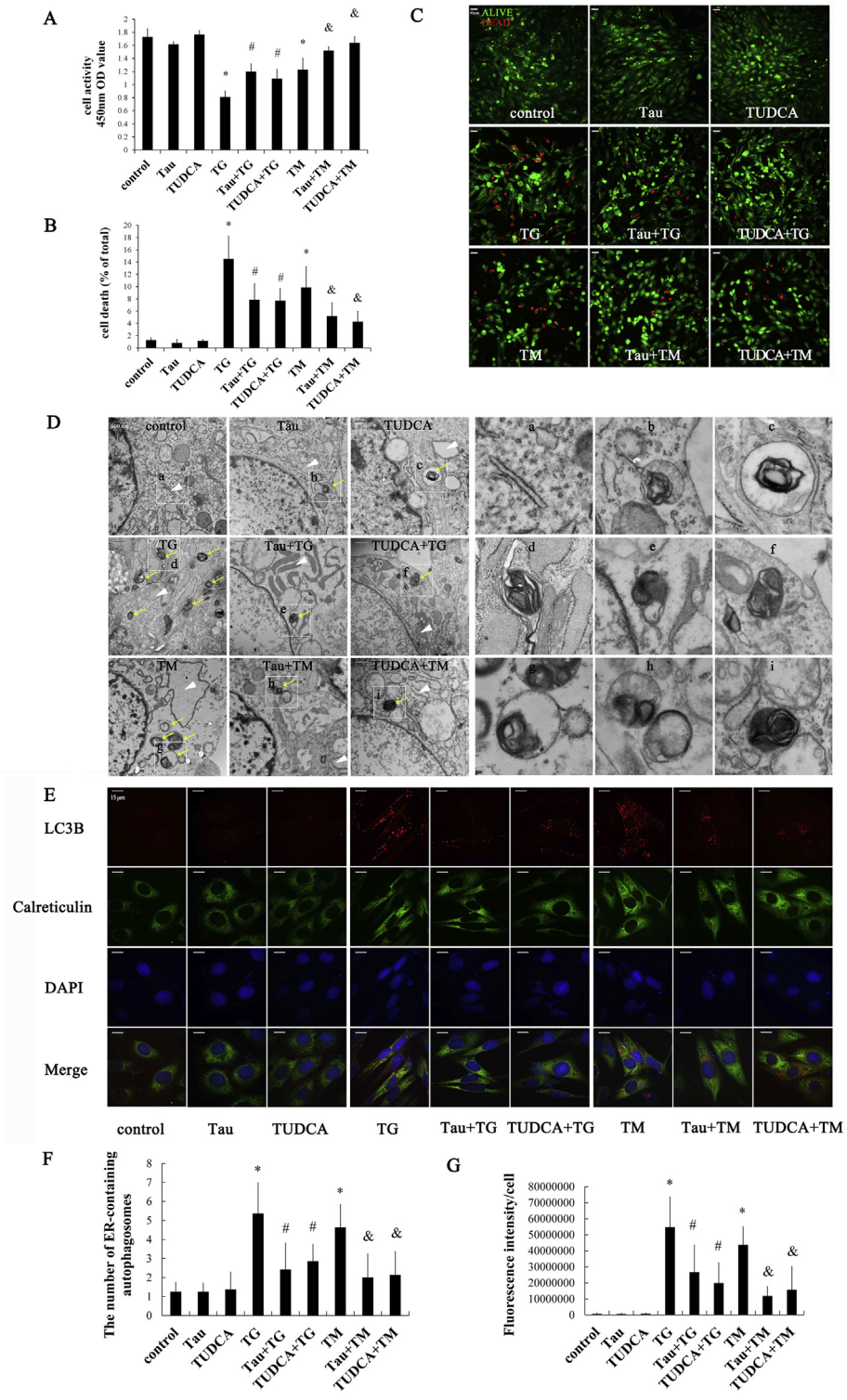

Fig. 2. Effect of ERS inhibitors (Tau or TUDCA) on cell viability, cell death and ER-phagy after TG or TM treatment in H9c2 cardiomyoblasts. (A) The viability of H9c2 cardiomyoblasts was detected with a CCK-8 assay. (B) Live or dead staining of H9c2 cardiomyoblasts was performed with a LIVE/DEAD® Viability/Cytotoxicity Kit. Quantitative analysis of live and dead H9c2 cardiomyoblasts is shown in (C). (C) Live cells are indicated by green staining and dead cells are indicated by red staining in confocal microscopy images (bar = 40 μm). (D) The effect of Tau or TUDCA on ER ultrastructure and ER-phagy after treatment with TG or TM was observed with transmission electron microscopy (bar = 500 nm). White arrows refer to the ER, and yellow arrows refer to ER-containing autophagosomes (ERAs). Panels a–i show amplified regions of the panels with ERAs, control to TUDCA + TM. (E) Representative confocal images of colocalization of LC3B and the ER (green, *anti*-calreticulin) in H9c2 cardiomyoblasts (bar = 15 μm). (F) The effects of Tau or TUDCA on ER-phagy induced by TG or TM were detected by the number of ERAs per cell. (G) The effects of Tau or TUDCA on ER-phagy after treatment with TG or TM were detected with the total fluorescence intensity of LC3B per cell. All experiments were done in triplicate. The data were analyzed via one-way analysis of variance and are expressed as the mean ± SD of three independent biological replicates in (A), (B), (F) and (G). $^{*}P < 0.05$ versus control, $^{\#}P < 0.05$ versus TG, $^{\&}P < 0.05$ versus TM. (For interpretation of the references to color in this figure legend, the reader is referred to the Web version of this article.)

treatment resulted in a 45.9% or 47.0% decrease in cell death compared with TG alone and a 47.4% or 56.9% decrease in cell death compared with TM alone ($P < 0.01$). These results suggest that ERS inhibitors decrease H9c2 cell injury induced by TG or TM.

ERS inhibitors attenuated ER-phagy induced by TG or TM in H9c2 cardiomyoblasts—To study the effect of ERS inhibitors on ER-phagy, the ultrastructure of H9c2 cardiomyoblasts was observed via transmission electron microscopy (Fig. 2D, F). TG or TM obviously induced ER expansion compared with controls (shown by the white triangle). Several ERAs with ER whorls (shown by the yellow arrow) appeared next to the ER. Compared with controls, the number of ERAs per cell in TG or TM group was increased by 3.3- or 2.7-fold, respectively ($P < 0.01$). After Tau or TUDCA treatment alone, the ER was slightly dilated, and autophagosomes were occasionally found, but the number of ERAs per cell in Tau or TUDCA group showed no difference compared with the control group. However, ERS inhibitors alleviated TG- or TM-induced ER expansion and ERAs compared with TG or TM alone. Tau or TUDCA decreased the number of ERAs treated with TG by 54.7% and 46.7% ($P < 0.01$) and downregulated the number of ERAs treated with TM by 56.9% and 53.8% ($P < 0.01$), respectively.

Immunofluorescence staining was used to detect the subcellular localization of LC3B in the ER associated with the effect of ERS inhibitors on ER-phagy (Fig. 2E, G). The results indicated that ER-phagy was induced by TG or TM treatment, which led to LC3B aggregation into lumps with high fluorescence intensity in the ER. Compared with controls, the total fluorescence intensity of LC3B per cell in TG or TM group was increased by 73.6- or 58.6-fold, respectively ($P < 0.01$). The expression and distribution of LC3B in H9c2 cardiomyoblasts treated with Tau or TUDCA alone showed no significant difference compared with controls, but Tau or TUDCA significantly alleviated TG- or TM-induced ER-phagy, which was manifested by the decrease in LC3B accumulation in the ER. Tau or TUDCA followed by TG or TM treatment resulted in a 51.4% and 63.7% decrease in the total fluorescence intensity of LC3B per cell compared with the TG group ($P < 0.01$) and a 72.7% and 64.1% decrease compared with the TM group ($P < 0.01$), respectively. The results suggest that ERS inhibitors alleviate ER-phagy induced by TG or TM in H9c2 cardiomyoblasts.

3.3. ERS inhibitors alleviated ER-phagy by inhibiting the PERK/Nrf2 pathway

ERS inhibitors attenuated TG- or TM-induced PERK phosphorylation—Having determined the impact of ERS inhibitors on ER-phagy under TG or TM conditions, we sought to examine its role in the PERK pathway. Using immunoblot analysis, alterations in PERK phosphorylation and expression were detected (Fig. 3BC). PERK phosphorylation increased with TG or TM treatment by 252% or 173%, while PERK protein expression increased by 99.7% or 73.3%, respectively ($P < 0.01$ vs. control). Moreover, the ratio of phosphorylated PERK to total PERK protein was increased by 76.2% and 57.4% compared with controls ($P < 0.01$). However, TG-treated cells with Tau or TUDCA pretreatment showed a 57.3% or 66.3% decrease in PERK phosphorylation, a 50.3% or 56.5% decrease in PERK expression and a 14.0% or 22.4% decrease in the ratio of phosphorylated PERK to total PERK protein compared with the TG group ($P < 0.01$). TM-treated cells with Tau or TUDCA pretreatment induced a 59.7% or 61.9% decrease in PERK phosphorylation, a 52.2% or 49.2% decrease in PERK expression, and a 15.8% or 25.0% decrease in the ratio of phosphorylated PERK to total PERK protein compared with the TM group ($P < 0.01$). These data provide evidence that ERS inhibitors alleviate ER-phagy by downregulating PERK phosphorylation and expression.

ERS inhibitors attenuated TG- or TM-induced Nrf2 nuclear translocation—We next sought to investigate the downstream effector in the PERK pathway: Nrf2. Fluorescence microphotographs revealed that Nrf2 appeared with a predominantly uniform distribution in the cytosol in control cells (Fig. 3A). However, in TG- or TM-treated H9c2 cardiomyoblasts, Nrf2 aggregated in the nucleus and was distributed as a cluster. Although there was no difference in Nrf2 distribution following Tau or TUDCA treatment alone, Tau or TUDCA pretreatment with TG or TM alleviated Nrf2 accumulation in the nucleus. To further confirm the PERK-mediated Nrf2 nuclear accumulation, the Nrf2 protein level in the nucleus was detected via Western blot analysis (Fig. 3D). Nuclear Nrf2 protein levels increased by 100.4% or 85.3% following TG or TM treatment ($P < 0.01$). Tau or TUDCA treatment alone had no significant effect on nuclear Nrf2 protein levels ($P > 0.05$), but Tau or TUDCA treatment resulted in a significant 24.8% or 26.1% decrease in nuclear Nrf2 proteins compared with the TG group ($P < 0.01$) and a 28.8% or 34.5% decrease compared with the TM group ($P < 0.01$), respectively. These data suggest that ERS inhibitors alleviate ER-phagy by inhibiting Nrf2 nuclear translocation.

ERS inhibitors attenuated TG- or TM-induced ATF4 protein expression—We also detected the effect of ERS inhibitors on ATF4, a Nrf2 downstream molecule (Fig. 3E). Compared with controls, TG or TM upregulated ATF4 expression by 92.0% or 86.9% ($P < 0.01$). Although Tau or TUDCA treatment alone had no significant effect on ATF4 protein expression ($P > 0.05$), both Tau and TUDCA significantly decreased ATF4 expression in cells treated with TG or TM. Compared with the TG group, ATF4 protein decreased by 25.0% in the Tau + TG group and 25.4% in the TUDCA + TG group ($P < 0.01$). Compared with the TM group, ATF4 protein decreased by 23.5% in the Tau + TM group and 34.7% in the TUDCA + TM group ($P < 0.01$). These results suggest that ERS inhibitors attenuate ER-phagy by downregulating ATF4 expression.

ERS inhibitors attenuated TG- or TM-induced Beclin 1 and LC3B-II protein expression—Alterations in Beclin 1 protein after treatment of H9c2 cardiomyoblasts with ERS inducers and inhibitors were detected via Western blot analysis. As shown in Fig. 3F, TG or TM increased Beclin 1 protein levels by 209% or 131% compared with the control group, respectively ($P < 0.01$), suggesting that both TG and TM induced autophagy. Although Beclin 1 protein levels in the Tau or TUDCA groups increased by 39.2% or 40.0% compared with controls ($P < 0.01$), both Tau and TUDCA decreased the TG- or TM-induced upregulation of Beclin 1 protein ($P < 0.01$). Compared with the TG group, Beclin 1 protein levels decreased by 36.5% in the Tau + TG group and 40.9% in the TUDCA + TG group ($P < 0.01$). Compared with the TM group, Beclin 1 protein levels decreased by 44.2% in the Tau + TM group and 38.3% in the TUDCA + TM group ($P < 0.01$). These results indicate that ERS inhibitors indirectly decrease expression of the autophagy-related molecule Beclin 1 through ATF4 activation.

We also detected the effect of ERS inhibitors on LC3B-II, a direct downstream effector of ATF4 (Fig. 3G). Under TG or TM conditions, LC3B-II protein levels increased by 105% or 198% compared with the control group ($P < 0.01$). Although there was no significant difference in LC3B-II protein levels between the control cells and cells treated with Tau or TUDCA ($P > 0.05$), Tau or TUDCA treatment followed by TG treatment resulted in a 37.9% or 21.3% decrease in LC3B-II protein compared with TG alone ($P < 0.01$). Moreover, Tau or TUDCA treatment followed by TM treatment resulted in a 34.1% or 42.3% decrease in LC3B-II protein compared with TM alone ($P < 0.01$). These data indicate that ERS inhibitors decrease the LC3B-II protein level, which plays an important role in ER-phagy.

3.4. Nrf2 inhibition alleviated PERK-mediated ER-phagy

To further confirm that Nrf2 plays a crucial role in PERK-mediated ER-phagy, we used the Nrf2 inhibitor all-trans retinoic acid (ATRA) [23,24] to explore the effect of Nrf2 nuclear translocation on ER-phagy.

Nrf2 inhibition attenuated TG- or TM-induced H9c2 cell injury—We detected H9c2 cell viability to estimate the effect of ATRA, a Nrf2 nuclear translocation inhibitor (Fig. 4A). TG or TM treatment induced a 51.9% or 35.0% decrease in cell viability compared with controls, respectively ($P < 0.01$). ATRA treatment prior to TG or TM treatment attenuated TG- or TM-induced cell injury, increasing cell viability by 21.8% in the ATRA + TG group compared with the TG group and 16.5% in the ATRA + TM group compared with the TM group ($P < 0.01$), although there was not a significant difference in the ATRA group ($P > 0.05$ vs. control).

We also detected cell death in H9c2 cardiomyoblasts after ATRA treatment (Fig. 4BC). TG or TM induced increased cell death by 9.2- or 6.4-fold compared with controls ($P < 0.01$). There was no difference in cell death after treatment with ATRA alone compared with controls. However, ATRA attenuated TG- or TM-induced H9c2 cell death, as shown by the 34.1% decrease in the ATRA + TG group compared with the TG group and the 40.8% decrease in the ATRA + TM group compared with the TM group ($P < 0.01$), suggesting that ATRA decreases TG- or TM-induced cell death by inhibiting Nrf2 nuclear translocation.

Nrf2 inhibition attenuated TG- or TM-induced ER-phagy—To investigate the effect of the Nrf2 inhibitor on ER-phagy, we detected LC3B localization in the ER via immunofluorescence staining as before (Fig. 4DE). The results showed that compared with the control group, LC3B accumulated as lumps in the ER and the total fluorescence intensity of LC3B per cell was significantly increased with TG or TM

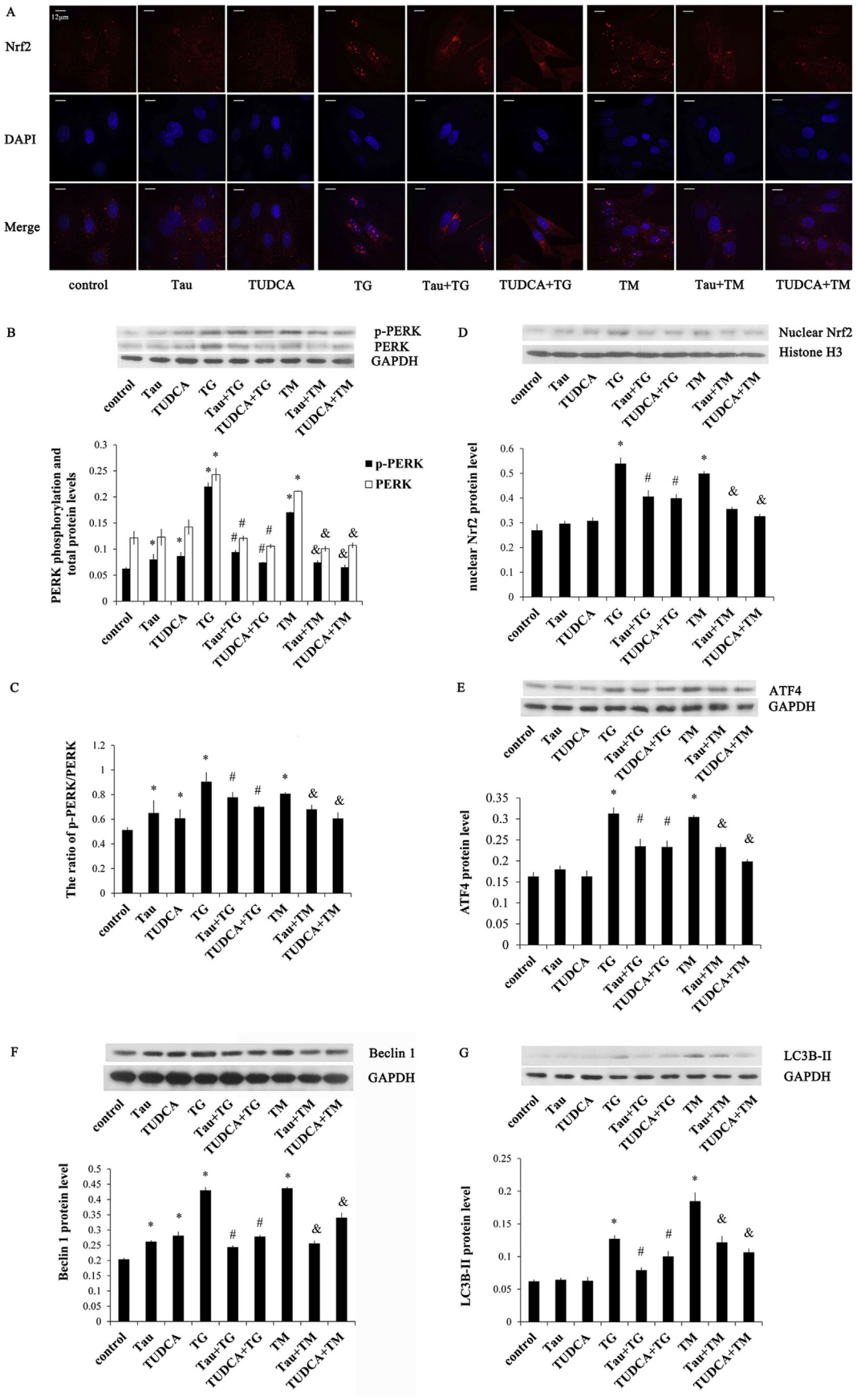

(caption on next page)

Fig. 3. ERS inhibitors attenuated ERS-related ER-phagy by inhibiting the PERK/Nrf2 pathway. (A) The subcellular distribution of Nrf2 was detected by immunofluorescence and laser scanning confocal microscopy (bar = 12 μm). (B–G) H9c2 cell homogenates were resolved via polyacrylamide gel electrophoresis, and protein levels were detected from total protein by western blotting using specific anti-PERK, *anti*-phospho-PERK (B and C), *anti*-ATF4 (E), *anti*-Beclin 1 (F) and *anti*-LC3B (G) antibodies. (D) The Nrf2 protein level was detected in the nuclear fraction by western blotting using a specific *anti*-Nrf2 antibody. GAPDH and histone H3 were used as normalization controls. The data were analyzed via one-way analysis of variance. Statistical significance was measured as standard deviation (SD) in (B) to (G), and each condition was assessed in three independent experiments. $^{*}P < 0.05$ versus control, $^{\#}P < 0.05$ versus TG, $^{\&}P < 0.05$ versus TM.

treatment. Although the distribution of LC3B in H9c2 cardiomyoblasts treated with ATRA alone exhibited no differences compared with controls, ATRA significantly decreased TG- or TM-induced LC3B accumulation in the ER. ATRA pretreatment showed a significant 68.3% decrease in the total fluorescence intensity of LC3B per cell compared with the TG group ($P < 0.01$) and a 56.2% decrease compared with the TM group ($P < 0.01$), respectively, suggesting that Nrf2 inhibition attenuated ER-phagy induced by TG or TM.

Nrf2 inhibition attenuated TG- or TM-induced Nrf2 nuclear translocation—The effect of the Nrf2 inhibitor on TG- or TM-induced Nrf2 nuclear translocation was examined by immunofluorescence staining (Fig. 4F). Compared with the control group, TG or TM treatment resulted in a redistribution of Nrf2 from a uniform distribution in the cytosol to a punctate distribution in the nucleus. In the ATRA group, Nrf2 showed no significant change in subcellular distribution compared with controls. However, ATRA combined with TG or TM treatment resulted in a decrease in Nrf2 punctate distribution in the nucleus, which suggests that ATRA pretreatment effectively inhibited ERS-induced Nrf2 nuclear translocation.

Nrf2 inhibition decreased TG- or TM-induced ATF4 protein expression—The effect of ATRA on ATF4 expression, a molecule downstream of Nrf2, was further detected (Fig. 4G). ATF4 expression was upregulated by TG or TM treatment, with an increase of 134.4% or 98.0% compared with controls ($P < 0.01$). Although ATRA treatment alone had no significant effect on ATF4 protein expression ($P > 0.05$), ATRA pretreatment significantly decreased TG- or TM-induced ATF4 expression, shown by the 28.1% decrease in the ATRA + TG group compared with the TG group and the 32.8% decrease in the ATRA + TM group compared with the TM group ($P < 0.01$), indicating that ATRA decreased TG- or TM-induced ATF4 expression by inhibiting Nrf2 nuclear translocation.

Nrf2 inhibition attenuated TG- or TM-induced Beclin 1 and LC3B-II

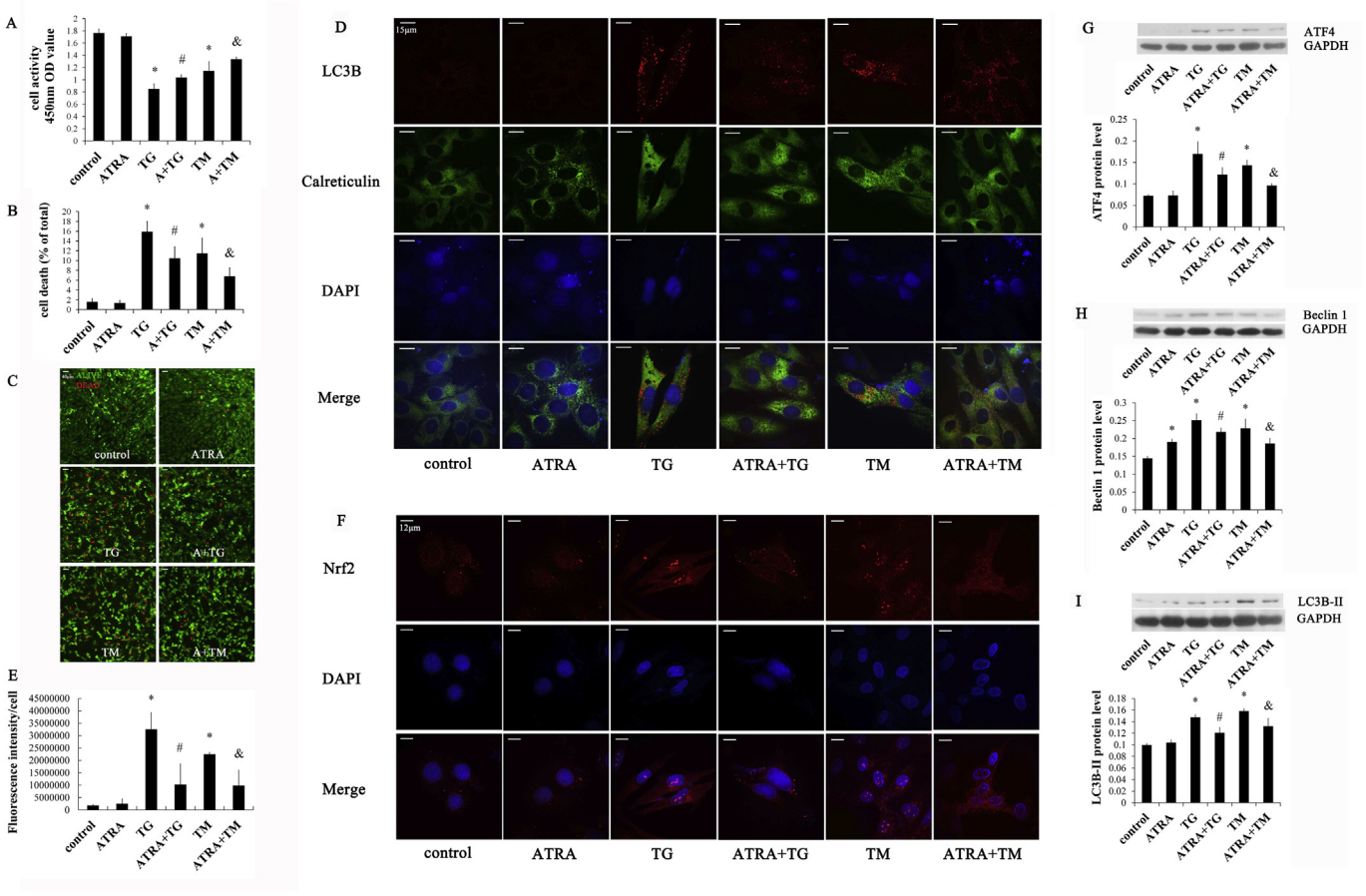

Fig. 4. Nrf2 inhibition attenuated TG- or TM-treated cell viability, cell death and ER-phagy in H9c2 cardiomyoblasts. (A) Cellular viability was detected with a CCK-8 assay. (B) Quantitative analysis of live and dead cells as shown in (C). (C) Live or dead cells were detected with a LIVE/DEAD® Viability/Cytotoxicity Kit (with green staining indicating live cells, and red staining indicating dead cells) and observed using a confocal microscope (bar = 40 μm). (D) Under a laser scanning confocal microscope, LC3B and calreticulin in H9c2 cardiomyoblasts were observed via immunofluorescence (bar = 15 μm). (E) The effect of Nrf2 inhibitor on ER-phagy after treatment with TG or TM was detected with the total fluorescence intensity of LC3B per cell. (F) Subcellular distribution of Nrf2 in H9c2 cardiomyoblasts was observed using immunofluorescence microscopy (bar = 12 μm). (G–I) Protein levels were resolved via SDS-PAGE and detected by western blotting using specific *anti*-ATF4 (G), *anti*-Beclin 1 (H) and *anti*-LC3B (I) antibodies. GAPDH was used as a normalization control. Densitometry was used to quantitate protein levels. The data were processed via one-way analysis of variance. Statistical significance was measured as standard deviation (SD), and each condition was assessed in three independent experiments. $^{*}P < 0.05$ versus control, $^{\#}P < 0.05$ versus TG, $^{\&}P < 0.05$ versus TM.

protein expression—Western blotting was used to detect the effect of the Nrf2 inhibitor on ERS-induced Beclin 1 protein upregulation. As shown in Fig. 4H, the Beclin 1 protein level increased by 73.7% or 57.8% under TG or TM conditions ($P < 0.01$ vs. control). Although ATRA treatment alone increased Beclin 1 protein levels by 31.3% compared with controls ($P < 0.01$), ATRA treatment followed by TG treatment decreased Beclin 1 protein levels by 13.1% compared with the TG group ($P < 0.01$). Moreover, ATRA treatment followed by TM treatment decreased Beclin 1 protein levels by 18.6% compared with the TM group ($P < 0.01$), suggesting that Nrf2 inhibition alleviated TG- or TM-induced autophagy by downregulating Beclin 1 protein expression.

In addition, the LC3B-II protein level was detected via Western blot analysis to investigate the effect of the Nrf2 inhibitor on the LC3B-II protein level (Fig. 4I). Compared with the control group, LC3B-II protein levels in the TG or TM treatment group were upregulated by 48.4% or 58.9%, respectively ($P < 0.01$). Although the LC3B-II protein level exhibited no difference between the ATRA group and the control group ($P > 0.05$), ATRA obviously decreased the LC3B-II protein levels after treatment with TG or TM by 18.2% or 16.6% compared with the TG or TM group, respectively ($P < 0.01$). These data provide further evidence that Nrf2 inhibition downregulated LC3B-II protein, an ER-phagy-related molecule, to inhibit TG- or TM-induced ER-phagy.

4. Discussion

Autophagy is a metabolic process in which lysosome-mediated intracellular proteins and organelles are degraded to maintain cellular homeostasis. Cardiovascular autophagy is involved in the occurrence, development and prognosis of cardiovascular disease [31]. Recent studies have revealed that in autophagy specific proteins or organelles are selectively engulfed. ER-phagy is selective autophagy that eliminates portions of the ER [3]. Suppression of ER-phagy, which was triggered by cadmium telluride-quantum dots (CdTe-QDs) in human embryonic kidney (HEK) cells, was previously shown to restore cell viability [9], indicating that inhibiting ER-phagy might have a protective effect on cells. In our study, ER-phagy and cell injury were induced independently by ERS inducers, namely, TG or TM, and ERS was inhibited by taurine and TUDCA. PERK-mediated Nrf2 nuclear translocation was suppressed by a Nrf2 inhibitor (ATRA). Thus, this study showed for the first time that the PERK/Nrf2 pathway is involved in ER-phagy as well as H9c2 cell injury. ERS inhibitors (Tau and TUDCA) and a Nrf2 nuclear translocation inhibitor (ATRA) suppressed the activation of the PERK/Nrf2 pathway induced by TG and TM, thereby alleviating ER-phagy and protecting H9c2 cardiomyoblasts from ERS-induced injury.

The mechanism underlying ER-phagy in H9c2 cardiomyoblasts has not been fully elucidated. ERS is an initially conserved cell stress response that establishes a communication axis between the ER and the nucleus, Golgi and mitochondria and maintains the balance between restoration of cellular homeostasis and apoptosis [10]. When ERS is excessive, ER-related apoptosis is initiated. Recent studies have indicated that ERS not only induces apoptosis but also mediates ER-phagy with the formation of ERAs [6]. Using electron microscopy, Schuck et al. observed ER membrane twisting as whorls in ERAs, which was thus named ER whorls [29]. Knocking out the autophagy-related gene Atg8/LC3 inhibited ERA formation. Further studies found that LC3B interacted with the ER-resident receptor FAM134B [11] and then specifically recognized and recruited ER membrane into autophagosomes, causing ER-phagy [12]. Rubio et al. detected ER-phagy by observing subcellular co-localization of LC3B and the ER marker calreticulin [30]. In this study, we used two ERS inducers to induce ERS-related ER-phagy: TG, which depletes Ca^{2+} from the ER, and TM, which inhibits protein N-linked glycosylation [25]. Calreticulin (CRT) is a Ca^{2+}-binding protein and a molecular chaperone in the ER that regulates ER homeostasis. ERS induced by Ca^{2+} overload or abnormal protein synthesis usually exhibits an upregulation of ERS-related molecules, such as CRT [28]. In our study, treatment with 20 nmol/L TG or 160 ng/mL TM for 48 h induced excessive ERS and injury, with an increase in the CRT protein level, a decrease in cell viability and an increase in cell death. The ultrastructure of H9c2 cardiomyoblasts showed that the number of ERAs increased in the TG or TM groups based on transmission electron microscopy observation. We found obvious ER whorls with a diameter of approximately 200–400 nm in ERAs, which was consistent with previous reports [6,29]. Immunofluorescence staining analysis showed that LC3B was localized in the ER of H9c2 cardiomyoblasts and aggregated into clumps with TG or TM treatment, suggesting that TG or TM initiated ER-phagy in H9c2 cardiomyoblasts. TUDCA is a chemical molecular chaperone in the ER that binds to the hydrophobic region of unfolded proteins to prevent their aggregation and inhibits ERS [21,22]. Taurine is also an ERS inhibitor [20] and significantly inhibits myocardial injury caused by excessive ERS [32]. In our study, ERS inhibitors (TUDCA and taurine) significantly alleviated ER-phagy induced by ERS, evidenced by the obviously decreased number of ERAs with ER whorls and by the accumulation of LC3B in the ER compared with TG or TM alone, as well as the decrease in CRT expression induced by TG or TM. Our data indicate that ERS activates ER-phagy and cell injury and ERS inhibitors protect H9c2 cardiomyoblasts by attenuating ER-phagy; however, the mechanism underlying ERS-induced ER-phagy should be further studied.

The early ERS response is dependent on the PERK pathway [10]. PERK activates its downstream target eIF2α and then selectively upregulates ATF4 translation. In addition, the PERK pathway is involved in the entire autophagy process: induction, vesicle nucleation, elongation and maturation. Beclin 1 is a core component of the class III PI 3-kinase (PI3K) complex, which is the initiator of autophagy [33]. LC3B is the key factor that mediates selective autophagy to degrade the ER. Thus, detection of LC3B-II protein, located on the surface of autophagosomes, is an effective method to evaluate ER-associated autophagy [34]. The PERK/ATF4-mediated downstream target CHOP was reported to upregulate BH3-only proteins, displacing Bcl-2/Bcl-XL from the BH3 domain of Beclin 1 to promote PI3K complex activation and autophagic vesicle nucleation. In addition, PERK-mediated ATF4 transcriptionally upregulates LC3B, which regulates ER-phagy-related vesicle elongation and maturation [11], suggesting that the PERK pathway might be critical for regulating ER-phagy. A recent study reported that knockdown of IRE1α induced autophagy by activating the PERK pathway but decreased the protein level of eIF2α, the classic downstream molecule of PERK [14], suggesting that there might be other targets that regulate PERK-mediated ER-phagy. Nrf2 is located in the cytoplasmic cytoskeleton during unstressed conditions. When oxidative stress occurs, Nrf2 translocates to the nucleus and binds to the antioxidant response element to initiate transcription of genes encoding antioxidant proteins and enzymes [15]. Recent studies have confirmed that Nrf2 is also an important downstream target of PERK. PERK phosphorylation activates Nrf2 nuclear translocation [10]. Others have found that continuous accumulation of Nrf2 in the nucleus causes cell damage. In Keap l knockout mice, Nrf2 aggregated in the nucleus of liver cells, resulting in severe liver damage [35]. Further studies showed that Nrf2 binds to the promoter of the ATF4 gene, and Nrf2 overexpression upregulated while Nrf2 knockdown downregulated ATF4 transcription in ARPE-19/HPV-16 cells [16], suggesting that Nrf2 could promote ATF4 transcription. In addition, knockdown of Nrf2 followed by oxidized phospholipids treatment in endothelial cells also significantly decreased ATF4 protein expression [17], suggesting that Nrf2 also regulates ATF4 translation. Our data suggest that the PERK/Nrf2/ATF4 pathway regulates ER-phagy through upregulation of LC3B-II and Beclin 1 proteins.

In our study, TG and TM induced PERK phosphorylation, Nrf2 nuclear translocation and ATF4 expression, and then upregulated ATF4 downstream LC3B-II and Beclin 1 protein levels. ERS inhibitors (Tau and TUDCA) inhibited Nrf2 nuclear translocation and decreased ATF4, LC3B-II and Beclin 1 protein levels by downregulating PERK phosphorylation, suggesting that ERS inhibitors could attenuate ER-phagy

by inhibiting activation of the PERK pathway in ERS. Furthermore, we treated H9c2 cardiomyoblasts with a Nrf2 nuclear translocation inhibitor (ATRA) [23,24]. Our results showed that ATRA treatment alone had no significant effect on Nrf2 or ATF4 expression, but ATRA prior to TG or TM treatment inhibited Nrf2 nuclear translocation induced by TG or TM and downregulated the protein levels of ATF4, LC3B-II and Beclin 1, thereby increasing cell viability and alleviating ER-phagy and cell death. These results indicate that Nrf2 nuclear translocation mediates ER-phagy by promoting expression of its downstream effector ATF4. Moreover, inhibition of the Nrf2/ATF4 pathway attenuates ER-phagy and protects H9c2 cardiomyoblasts from ERS-induced injury.

5. Conclusion

In conclusion, we demonstrate that ERS induced H9c2 cell injury through excessive ER-phagy. The PERK pathway mediates ERS-induced ER-phagy by upregulating Nrf2 nuclear translocation and induces ATF4 expression, leading to upregulating of LC3B and Beclin 1 proteins to promote the formation and maturation of ERAs. Our findings suggest the potential mechanism of ERS-induced ER-phagy, thus providing new insights into the development of novel therapeutic strategies for cardiovascular disease.

Declaration of competing interest

The authors declare that there are no conflicts of interest.

Acknowledgments

This work was supported by the National Natural Science Foundation of China (grant numbers 31771287 and 31971049) and the National Basic Research Program of China (grant number 2015CB554405).

References

[1] C.W. Yancy, M. Jessup, B. Bozkurt, J. Butler, D.E. Casey Jr., M.M. Colvin, M.H. Drazner, G.S. Filippatos, G.C. Fonarow, M.M. Givertz, S.M. Hollenberg, J. Lindenfeld, F.A. Masoudi, P.E. McBride, P.N. Peterson, L.W. Stevenson, C. Westlake, 2017 ACC/AHA/HFSA focused update of the 2013 ACCF/AHA guideline for the management of heart failure: a report of the American college of cardiology/American heart association task force on clinical practice guidelines and the heart failure society of America, J. Card. Fail. 23 (2017) 628–651, https://doi.org/10.1016/j.cardfail.2017.04.014.

[2] J. Mialet-Perez, C. Vindis, Autophagy in health and disease: focus on the cardiovascular system, Essays Biochem. 61 (2017) 721–732, https://doi.org/10.1042/EBC20170022.

[3] S. Bernales, S. Schuck, P. Walter, ER-phagy: selective autophagy of the endoplasmic reticulum, Autophagy 3 (2007) 285–287, https://doi.org/10.4161/auto.3930.

[4] G. Ashrafi, T.L. Schwarz, The pathways of mitophagy for quality control and clearance of mitochondria, Cell Death Differ. 20 (2013) 31–42, https://doi.org/10.1038/cdd.2012.81.

[5] C. Ward, N. Martinez-Lopez, E.G. Otten, B. Carroll, D. Maetzel, R. Singh, S. Sarkar, V.I. Korolchuk, Autophagy, lipophagy and lysosomal lipid storage disorders, Biochim. Biophys. Acta 1861 (2016) 269–284, https://doi.org/10.1016/j.bbalip.2016.01.006.

[6] S. Bernales, K.L. McDonald, P. Walter, Autophagy counterbalances endoplasmic reticulum expansion during the unfolded protein response, PLoS Biol. 4 (2006) e423, https://doi.org/10.1371/journal.pbio.0040423.

[7] E. Cebollero, F. Reggiori, C. Kraft, Reticulophagy and ribophagy: regulated degradation of protein production factories, Int. J. Cell Biol. 2012 (2012) 182834, https://doi.org/10.1155/2012/182834.

[8] R.A. Hanna, M.N. Quinsay, A.M. Orogo, K. Giang, S. Rikka, A.B. Gustafsson, Microtubule-associated protein 1 light chain 3 (LC3) interacts with Bnip3 protein to selectively remove endoplasmic reticulum and mitochondria via autophagy, J. Biol. Chem. 287 (2012) 19094–190104, https://doi.org/10.1074/jbc.M111.322933.

[9] S. Jiang, Y. Lin, H. Yao, C. Yang, L. Zhang, B. Luo, Z. Lei, L. Cao, N. Lin, X. Liu, Z. Lin, C. He, The role of unfolded protein response and ER-phagy in quantum dots-induced nephrotoxicity: an in vitro and in vivo study, Arch. Toxicol. 92 (2018) 1421–1434, https://doi.org/10.1007/s00204-018-2169-0.

[10] C. Hetz, The unfolded protein response: controlling cell fate decisions under ER stress and beyond, Nat. Rev. Mol. Cell Biol. 13 (2012) 89–102, https://doi.org/10.1038/nrm3270.

[11] A. Khaminets, T. Heinrich, M. Mari, P. Grumati, A.K. Huebner, M. Akutsu, L. Liebmann, A. Stolz, S. Nietzsche, N. Koch, M. Mauthe, I. Katona, B. Qualmann, J. Weis, F. Reggiori, I. Kurth, C.A. Hübner, I. Dikic, Regulation of endoplasmic reticulum turnover by selective autophagy, Nature 522 (2015) 354–358, https://doi.org/10.1038/nature14498.

[12] S. Song, J. Tan, Y. Miao, Q. Zhang, Crosstalk of ER stress-mediated autophagy and ER-phagy: involvement of UPR and the core autophagy machinery, J. Cell. Physiol. 233 (2018) 3867–3874, https://doi.org/10.1002/jcp.26137.

[13] S. Deegan, S. Saveljeva, A.M. Gorman, A. Samali, Stress-induced self-cannibalism: on the regulation of autophagy by endoplasmic reticulum stress, Cell, Mol. Life Sci. 70 (2013) 2425–2441, https://doi.org/10.1007/s00018-012-1173-4.

[14] A. Storniolo, V. Alfano, S. Carbotta, E. Ferretti, L. Di Renzo, IRE1α deficiency promotes tumor cell death and eIF2α degradation through PERK dependent autophagy, Cell Death Dis. 4 (2018) 19, https://doi.org/10.1038/s41420-018-0082-1.

[15] M.C. Lu, J.A. Ji, Z.Y. Jiang, Q.D. You, The Keap1-Nrf2-ARE pathway as a potential preventive and therapeutic target: an update, Med. Res. Rev. 36 (2016) 924–963, https://doi.org/10.1002/med.21396.

[16] N. Miyamoto, H. Izumi, R. Miyamoto, H. Bin, H. Kondo, A. Tawara, Y. Sasaguri, K. Kohno, Transcriptional regulation of activating transcription factor 4 under oxidative stress in retinal pigment epithelial ARPE-19/HPV-16 cells, Investig. Ophthalmol. Vis. Sci. 52 (2011) 1226–1234, https://doi.org/10.1167/iovs.10-5775.

[17] T. Afonyushkin, O.V. Oskolkova, M. Philippova, T.J. Resink, P. Erne, B.R. Binder, V.N. Bochkov, Oxidized phospholipids regulate expression of ATF4 and VEGF in endothelial cells via NRF2-dependent mechanism: novel point of convergence between electrophilic and unfolded protein stress pathways, Arterioscler. Thromb. Vasc. Biol. 30 (2010) 1007–1013, https://doi.org/10.1161/ATVBAHA.110.204354.

[18] S.J. Watkins, G.M. Borthwick, H.M. Arthur, The H9C2 cell line and primary neonatal cardiomyocyte cells show similar hypertrophic responses in vitro, In Vitro Cell. Dev. Biol. Anim. 47 (2011) 125–131, https://doi.org/10.1007/s11626-010-9368-1.

[19] Z.Y. Zhang, X.H. Liu, W.C. Hu, F. Rong, X.D. Wu, The calcineurin-myocyte enhancer factor 2c pathway mediates cardiac hypertrophy induced by endoplasmic reticulum stress in neonatal rat cardiomyocytes, Am. J. Physiol. Heart Circ. Physiol. 298 (2010) H1499–H1509, https://doi.org/10.1152/ajpheart.00980.2009.

[20] M. Liu, M. Xue, X.R. Wang, T.Q. Tao, F.F. Xu, X.H. Liu, D.Z. Shi, Panax quinquefolium saponin attenuates cardiomyocyte apoptosis induced by thapsigargin through inhibition of endoplasmic reticulum stress, J. Geriatr. Cardiol. 12 (2015) 540–546, https://doi.org/10.11909/j.issn.1671-5411.2015.05.009.

[21] S.D. Miller, C.M. Greene, C. McLean, M.W. Lawless, C.C. Taggart, S.J. O'Neill, N.G. McElvaney, Tauroursodeoxycholic acid inhibits apoptosis induced by Z alpha-1 antitrypsin via inhibition of Bad, Hepatology 46 (2007) 496–503, https://doi.org/10.1002/hep.21689.

[22] A.R. Gani, J.K. Uppala, K.V. Ramaiah, Tauroursodeoxycholic acid prevents stress induced aggregation of proteins in vitro and promotes PERK activation in HepG2 cells, Arch. Biochem. Biophys. 568 (2015) 8–15, https://doi.org/10.1016/j.abb.2014.12.031.

[23] S. Ding, X. Hou, J. Yuan, X. Tan, J. Chen, N. Yang, Y. Luo, Z. Jiang, P. Jin, Z. Dong, L. Feng, X. Jia, Wedelolactone protects human bronchial epithelial cell injury against cigarette smoke extract-induced oxidant stress and inflammation responses through Nrf2 pathway, Int. Immunopharmacol. 29 (2015) 648–655, https://doi.org/10.1016/j.intimp.2015.09.015.

[24] S. Jayakumar, D. Pal, S.K. Sandur, Nrf2 facilitates repair of radiation induced DNA damage through homologous recombination repair pathway in a ROS independent manner in cancer cells, Mutat. Res. 779 (2015) 33–45, https://doi.org/10.1016/j.mrfmmm.2015.06.007.

[25] F. Foufelle, B. Fromenty, Role of endoplasmic reticulum stress in drug-induced toxicity, Pharmacol. Res. Perspect. 4 (2016) e00211, , https://doi.org/10.1002/prp2.211.

[26] F. Wang, T. Pulinilkunnil, S. Flibotte, C. Nislow, I. Vlodavsky, B. Hussein, B. Rodrigues, Heparanase protects the heart against chemical or ischemia/reperfusion injury, J. Mol. Cell. Cardiol. 131 (2019) 29–40, https://doi.org/10.1016/j.yjmcc.2019.04.008.

[27] Y. Yu, G. Sun, Y. Luo, M. Wang, R. Chen, J. Zhang, Q. Ai, N. Xing, X. Sun, Cardioprotective effects of Notoginsenoside R1 against ischemia/reperfusion injuries by regulating oxidative stress- and endoplasmic reticulum stress- related signaling pathways, Sci. Rep. 6 (2016) 21730, https://doi.org/10.1038/srep21730.

[28] B.Y. Owusu, K.A. Zimmerman, J.E. Murphy-Ullrich, The role of the endoplasmic reticulum protein calreticulin in mediating TGF-β-stimulated extracellular matrix production in fibrotic disease, J. Cell Commun. Signal. 12 (2018) 289–299, https://doi.org/10.1007/s12079-017-0426-2.

[29] S. Schuck, C.M. Gallagher, P. Walter, ER-phagy mediates selective degradation of endoplasmic reticulum independently of the core autophagy machinery, J. Cell Sci. 127 (2014) 4078–4088, https://doi.org/10.1242/jcs.154716.

[30] N. Rubio, I. Coupienne, E. Di Valentin, I. Heirman, J. Grooten, J. Piette, P. Agostinis, Spatiotemporal autophagic degradation of oxidatively damaged organelles after photodynamic stress is amplified by mitochondrial reactive oxygen species, Autophagy 8 (2012) 1312–1324, https://doi.org/10.4161/auto.20763.

[31] O. Yamaguchi, Autophagy in the heart, Circ. J. 83 (2019) 697–704, https://doi.org/10.1253/circj.CJ-18-1065.

[32] M. Liu, X.R. Wang, C. Wang, D.D. Song, X.H. Liu, D.Z. Shi, Panax quinquefolium saponin attenuates ventricular remodeling after acute myocardial infarction by inhibiting chop-mediated apoptosis, Shock 40 (2013) 339–344, https://doi.org/10.1097/SHK.0b013e3182a3f9e5.

[33] S.F. Funderburk, Q.J. Wang, Z. Yue, The beclin l-vps34 complex—at the crossroads of autophagy and beyond, Trends Cell Biol. 20 (2010) 355–362, https://doi.org/10.1016/j.tcb.2010.03.002.

[34] E. Varghese, S.M. Samuel, S. Varghese, S. Cheema, R. Mamtani, D. Büsselberg, Triptolide decreases cell proliferation and induces cell death in triple negative MDA-MB-231 breast cancer cells, Biomolecules 8 (2018) E163, https://doi.org/10.3390/biom8040163.

[35] K. Taguchi, N. Fujikawa, M. Komatsu, T. Ishii, M. Unno, T. Akaike, H. Motohashi, M. Yamamoto, Keap1 degradation by autophagy for the maintenance of redox homeostasis, Proc. Natl. Acad. Sci. U.S.A. 109 (2012) 13561–13566, https://doi.org/10.1073/pnas.1121572109.